

Rapid multi-component phase-split calculations using volume functions and reduction methods

Mohamad Fathi*and Stefan Hickel†

Aerodynamics Group, Faculty of Aerospace Engineering, Delft University of
Technology
Kluyverweg 2, 2629 HS Delft, The Netherlands

Abstract

We present a new family of fast and robust methods for the calculation of the vapor-liquid equilibrium at isobaric-isothermal (PT-flash), isochoric-isothermal (VT-flash), isenthalpic-isobaric (HP-flash), and isoenergetic-isochoric (UV-flash) conditions. The framework is provided by formulating phase-equilibrium conditions for multi-component mixtures in an effectively reduced space based on the molar specific value of the recently introduced volume function derived from the Helmholtz free energy. The proposed algorithmic implementation can fully exploit the optimum quadratic convergence of a Newton method with the analytical Jacobian matrix. This paper provides all required exact analytic expressions for the general cubic equation of state. Computational results demonstrate the effectivity and efficiency of the new methods. Compared to conventional methods, the proposed reduced-space iteration leads to a considerable speed-up as well as to improved robustness and better convergence behavior near the spinodal and coexistence curves of multi-component mixtures, where the preconditioning by the reduction method is most effective.

Keywords: vapor-liquid equilibrium, reduction method, volume function, constant volume flash

1 Introduction

Robust, computationally efficient and accurate phase splitting or flash calculations play a crucial role in many engineering disciplines, such as chemical-process and reservoir simulations. In Com-

*email: m.fathi@tudelft.nl ; orcid: <https://orcid.org/0000-0001-9122-228X>

†email: s.hickel@tudelft.nl ; orcid: <https://orcid.org/0000-0002-7463-9531>

putational Fluid Dynamics (CFD) simulations of realistic multi-component vapor-liquid fluid flows, millions of phase equilibrium calculations are required every time step in the form of either the VT-flash or UV-flash, depending on the chosen formulation of the governing equations: The VT-flash is needed in cases where the overall specific volume, temperature and composition are known, such as for the carbon dioxide injection into subsurface reservoirs^{1,2}. Methods that solve the compressible Navier-Stokes equations based on the conservation laws for mass, linear momentum and total energy, such as applied for the simulation of the trans-critical vaporization of liquid fuels³⁻⁶, require a UV-flash, where the input is the overall specific internal energy, volume and composition. The calculation of thermodynamic equilibrium properties of multi-component multi-phase mixtures typically consumes more than three quarters of the total computational time^{7,8} and thus imposes severe limitation on the tractable space-time resolution or even the computational feasibility of such numerical simulations. At the same time, flash algorithms for CFD applications have to be fault tolerant and robust, because even a method that fails to converge only once in a billion will eventually spoil the entire simulation.

The simplest case and workhorse of most phase-equilibrium calculations is the so-called PT-flash, where the equilibrium pressure and temperature of the mixture are already given. Most methods for calculating the isobaric-isothermal equilibrium volume fractions and compositions follow the approach proposed by Michelsen^{9,10}. For solving flash problems at conditions other than constant pressure and temperature, Michelsen¹¹ introduced an indirect method based on nesting simple and robust PT-flash calculations. For VT-flashes, for example, Michelsen's method aims to find the pressure at which the PT-flash results in the given total specific volume. This results in an optimization algorithm, in which the pressure is adjusted in the outer loop and a PT-flash is solved in the inner loop. Accordingly, UV-flashes are solved by a bi-variant optimization of temperature and pressure corresponding to the given internal energy and volume, which define the thermodynamic state, for example, in mass and energy conservative Navier-Stokes solvers³.

Nested algorithms based on the PT-flash are also attractive for mixtures with many components, because they offer the possibility of adopting reduction methods¹², which provide a considerable speedup and, in addition, improve the robustness of the algorithm¹³. The first reduction method was introduced by Michelsen¹², who found that the phase-splitting problem is fully defined by only three reduced parameters regardless of the number of components when all Binary Interaction Coefficients (BICs) are zero. Hendriks and Van Bergen¹⁴ successfully generalized the method for cases with some non-zero BICs through an eigenvalue analysis of the binary interaction matrix. Nichita and Graciaa¹⁵ found a new set of reduced parameters for PT-flash calculations, for which

they demonstrated a notable decrease in the number of iterations relative to previous reduction methods specifically near the phase boundary and the critical point.

Employing a direct VT-flash, on the other hand, could considerably reduce the computational time by eliminating the outer pressure iteration loop, provided that the method itself would be fast and robust enough. To this end, Mikyška and Firoozabadi¹⁶ introduced an alternative formulation of the VT-flash problem based on a new thermodynamic function, the so-called volume function. They solved the problem directly by a successive-substitution iteration (SSI) algorithm with nearly the same number of iterations as a conventional PT-flash based solver requires for one inner iteration loop. Recently, Jindrová and Mikyška¹⁷ and Nichita¹⁸ presented methods for solving the VT-flash problem via direct minimization of the total Helmholtz free energy. Cismondi et al.¹⁹ directly included the pressure equality and volume constraint in a new algorithm very similar to the PT-flash, and showed about 20% reduction in the computational time compared to Michelsen's nested optimization technique. However, for working fluids with a large number of components, these methods lead to a significantly stronger increase of the computational time compared to the nested approach that benefits from the quadratic Newton-Raphson convergence rate in the reduced space.

Extending the work of Mikyška and Firoozabadi¹⁶ and Nichita and Graciaa¹⁵, we present a very fast and robust method for direct vapor-liquid phase-split calculations based on formulating phase equilibrium conditions in terms of the molar specific value of Mikyška and Firoozabadi's volume function (instead of fugacity coefficients) and a corresponding reduction method. This new formulation allows us to solve isothermal flashes (both PT and VT) directly and with the exact analytical Jacobian matrix, which results in optimum quadratic convergence of the Newton-Raphson method. Non-isothermal cases, such as UV and HP flashes, are solved through nested univariate optimization with the corresponding isothermal flash (PT for HP and VT for UV) and the readily available specific heat capacity at constant pressure (for HP-flash) or at constant volume (for UV-flash) as exact Jacobian.

This paper is structured as follows: First, the mathematical description of the equilibrium problem is reformulated based on the molar specific values of the volume function for the vapor and liquid phases. Next, the classical reduction method is presented along with the derivation of new reduced parameters in the context of the new formulations, and all other thermodynamic relations required for non-isothermal flashes are also derived from the reduced parameters. Then, algorithms based on the Newton-Raphson method with the analytical Jacobian matrix for the direct solution of isothermal flashes and for the indirect solution of non-isothermal ones, are presented. Last but not least, the reliability and efficiency of proposed algorithms and its significantly improved

computational performance compared to a recently published implementation for high-fidelity CFD simulations³ will be demonstrated and discussed for different multi-component mixtures at various thermodynamic conditions.

2 Thermodynamic equilibrium formulation

According to the Gibbsian thermodynamics²⁰, a multi-component system consisting of vapor and liquid phases is in equilibrium when the temperatures, pressures, and chemical potentials of phases are equal, that is,

$$T^L = T^V, \quad p^L = p^V, \quad \mu_i^L = \mu_i^V, \quad (1)$$

where T , p , and μ_i are temperature, pressure, and chemical potential of component $i = \{1 \dots n\}$ in a mixture with n components, and superscripts L and V refer to values of the liquid and vapor phases.

The pressures can be computed as a function of temperature, molar specific volume and composition of each phase using the general form of the cubic equation of states (EoS)

$$p = \frac{RT}{v - b} - \frac{a}{(v + \delta_1 b)(v + \delta_2 b)}, \quad (2)$$

where δ_1 and δ_2 are the two EoS parameters (see below), R is the universal gas constant, and v is the molar specific volume of the mixture. The energy and co-volume parameters a and b are usually computed using the van der Waals mixing rules

$$a = \sum_{i=1}^n \sum_{j=1}^n z_i z_j (1 - \kappa_{ij}) \sqrt{\hat{a}_i \hat{a}_j}, \quad (3)$$

and

$$b = \sum_{i=1}^n z_i \hat{b}_i, \quad (4)$$

in which z_i is the mole fraction of the component i , and κ_{ij} is the binary interaction coefficient between component i and j in the mixture. \hat{a}_i and \hat{b}_i are energy and co-volume parameters of the pure component i , which are obtained through

$$\hat{a}_i = \Omega_a \frac{R^2 T_{ci}^2}{p_{ci}} \left[1 + c(\omega_i) \left(1 - \sqrt{\frac{T}{T_{ci}}} \right) \right]^2 \quad (5)$$

and

$$\hat{b}_i = \Omega_b \frac{RT_{ci}}{p_{ci}}, \quad (6)$$

where T_{ci} , p_{ci} are critical temperature and pressure of the component i . The two constants Ω_a and Ω_b as well as the form of the function of $c(\omega_i)$, in which ω_i is the acentric factor, depend of the selected cubic EoS: for instance, in the Peng-Robinson (PR) EoS: $\delta_1 = 1 + \sqrt{2}$ and $\delta_2 = 1 - \sqrt{2}$, which result in $\Omega_a = 0.45724$, $\Omega_b = 0.0778$, and the functional $c(\omega_i)$ is:

$$c(\omega_i) = \begin{cases} 0.37464 + 1.54226\omega_i - 0.26992\omega_i^2 & , \text{ for } \omega_i < 0.5 \\ 0.3796 + 1.485\omega_i - 0.1644\omega_i^2 + 0.01667\omega_i^3 & , \text{ for } \omega_i \geq 0.5 \end{cases}.$$

In the Soave-Redlich-Kwong (SRK) EoS, with $\delta_1 = 0$ and $\delta_2 = 1$, they are $\Omega_a = 0.42748$, $\Omega_b = 0.08664$, and $c(\omega_i) = 0.48508 + 1.55171\omega_i - 0.15613\omega_i^2$.

The equality of chemical potentials is typically expressed in terms of the K-factor (also named K-value or equilibrium ratio, which is the ratio of the mole fractions in the vapor (y) and liquid (x) phases), and the fugacity coefficient derived from the Gibbs free energy. The logarithmic form of this relation for a two-phase vapor-liquid mixture is

$$\ln K_i = \ln \varphi_i^L - \ln \varphi_i^V, \text{ for } i = 1 \dots n, \quad (7)$$

with φ as the fugacity coefficient and K as the K-factor. Mikyška and Firoozabadi¹⁶ derived a new thermodynamic function for the evaluation of the equilibrium ratio via minimization of the Helmholtz free energy that uses the specific volume, temperature, and mole fractions as its primary variables and eliminates the need for knowing the equilibrium pressure and for solving the state equation for the stable volume. They proved that the following relationship exists between the K-factor and the volume function coefficient for the liquid and vapor phases:

$$K_i = \frac{v^V \Phi_i(v^V, T, y_1, \dots, y_n)}{v^L \Phi_i(v^L, T, x_1, \dots, x_n)}, \quad (8)$$

in which Φ_i is the volume function coefficient of the component i and can be computed analytically as a function of temperature, specific volume, and mole fractions via

$$\ln \Phi_i = \int_v^{+\infty} \left[\frac{1}{v} - \frac{1}{RT} \left(\frac{\partial p}{\partial z_i} \right)_{T, v, z_j \neq i} \right] dv. \quad (9)$$

We define

$$\psi_i \equiv v\Phi_i \quad (10)$$

as the molar specific value of the volume function, such that, instead of using Eq. (7), the natural logarithm of K-factors can be calculated by

$$\ln K_i = \ln \psi_i^V - \ln \psi_i^L, \text{ for } i = 1 \dots n. \quad (11)$$

It can be shown that this (molar) specific volume function is related to the fugacity coefficient via $\psi_i = RT/p\varphi_i$. By substituting the general cubic EoS (2) for the evaluation of the partial pressure term in the integral (9), the following expression is obtained for this new thermodynamic function:

$$\ln \psi_i = \ln(v-b) - \frac{\hat{b}_i}{v-b} + \frac{av\hat{b}_i/(bRT)}{(v+\delta_1b)(v+\delta_2b)} - \frac{a\hat{b}_i - 2bg_i}{(\delta_1 - \delta_2)b^2RT} \ln\left(\frac{v+\delta_1b}{v+\delta_2b}\right) \quad (12)$$

where g_i is

$$g_i = \sum_{j=1}^n z_j (1 - \kappa_{ij}) \sqrt{\hat{a}_i \hat{a}_j}, \text{ for } i = 1 \dots n. \quad (13)$$

The equality of chemical potentials and component material balances can be systematically expressed by means of K-factors in such a way that the vapor mole fraction θ is determined by the classic Rachford-Rice equation

$$\sum_{i=1}^n \frac{\hat{z}_i(K_i - 1)}{1 + \theta(K_i - 1)} = 0, \quad (14)$$

where \hat{z}_i is the overall mole fractions of component i in the feed. Then, molar compositions of the liquid and vapor phases are obtained:

$$x_i = \frac{\hat{z}_i}{1 + \theta(K_i - 1)} \quad \text{and} \quad y_i = x_i K_i, \quad \text{for } i = 1 \dots n. \quad (15)$$

This formulation leads to a remarkable reduction in the number of variables in isothermal flash calculations; we know the overall composition of the feed hence, by knowing the n K-factors, we can compute the molar compositions of the vapor and liquid. The molar specific volumes of phases can then be computed by evaluating the state equations separately for vapor and liquid based on the given pressure in PT-flash calculations²¹, or by solving the pressure equality equation along with a volume constraint based on the given volume in VT-flash calculations¹⁹.

3 Reduction method

The basic idea of all reduction methods is to calculate the K-factors in a lower-dimensional hyper-space spanned by parameters that are independent of the number of components in the mixture. According to the classical theory of reduction²⁰, such reduced parameters can be obtained by decomposing the symmetric matrix $\beta_{ij} = 1 - \kappa_{ij}$ that represents the binary interactions into matrices composed of its eigenvectors and eigenvalues, that is,

$$\beta = SDS^{-1} = SDS^T, \quad (16)$$

in which the diagonal matrix $D = \text{diag}(\lambda_1, \dots, \lambda_n)$ represents the eigenvalues $\lambda_i (i = 1 \dots n)$ of the matrix β , and the orthogonal matrix $S = (\vec{s}_1, \dots, \vec{s}_n)$ includes the corresponding eigenvectors $\vec{s}_i (i = 1 \dots n) = (s_{i1}, \dots, s_{in})^T$. For most mixtures with a large number of components, only a few ($m < n$) eigenvalues are significant as a result of negligible binary interactions between many components; we can hence use the following approximation for the evaluation of the entries of the matrix β :

$$\beta_{ij} = \sum_{k=1}^n \lambda_k s_{ki} s_{kj} \approx \sum_{k=1}^m \lambda_k s_{ki} s_{kj}. \quad (17)$$

Defining $\hat{s}_{ki} \equiv s_{ki} \sqrt{\hat{a}_i}$ as entries of the reduction matrix with size of $m \times n$, we can express $g_i (i = 1 \dots n)$ in Eq. (13) as

$$g_i = \sum_{j=1}^n z_j \left(\sum_{k=1}^m \lambda_k s_{ki} s_{kj} \right) \sqrt{\hat{a}_i \hat{a}_j} = \sum_{k=1}^m \lambda_k \hat{s}_{ki} \left(\sum_{j=1}^n z_j \hat{s}_{kj} \right) = \sum_{k=1}^m \lambda_k \hat{s}_{ki} q_k, \quad (18)$$

as a function of the reduced parameters

$$q_k = \sum_{i=1}^n z_i \hat{s}_{ki}, \text{ for } k = 1 \dots m. \quad (19)$$

Similarly, the energy parameter a of the mixture in Eq. (3) can be calculated from these reduced parameters via

$$a = \sum_{i=1}^n \sum_{j=1}^n z_i z_j \left(\sum_{k=1}^m \lambda_k s_{ki} s_{kj} \right) \sqrt{\hat{a}_i \hat{a}_j} = \sum_{k=1}^m \lambda_k \left(\sum_{i=1}^n z_i \hat{s}_{ki} \right)^2 = \sum_{k=1}^m \lambda_k q_k^2. \quad (20)$$

Then, an equation for evaluation of the molar specific value of the volume functions, ψ_i , can be derived by substituting $g_i (i = 1 \dots n)$ and a into Eq. (12) using Eqs. (18) and (20):

$$\ln \psi_i = \sum_{k=1}^m h_k \hat{s}_{ki} + h_{m+1} \hat{b}_i + h_{m+2} \quad , \text{ for } i = 1 \dots n, \quad (21)$$

where coefficients h are functions of $q_k (k = 1 \dots m)$, b , and v :

$$\begin{aligned} h_k &= 2\lambda_k q_k \ln [(v + \delta_1 b)/(v + \delta_2 b)] / [(\delta_1 - \delta_2)bRT] \quad , \text{ for } k = 1 \dots m \\ h_{m+1} &= \sum_{k=1}^m \lambda_k q_k^2 \left\{ \begin{array}{l} vb / [(v + \delta_1 b)(v + \delta_2 b)] - \\ \ln [(v + \delta_1 b)/(v + \delta_2 b)] / (\delta_1 - \delta_2) \end{array} \right\} / (RTb^2) - 1/(v - b), \quad (22) \\ h_{m+2} &= \ln(v - b). \end{aligned}$$

Because the entries of reduction matrix \hat{s}_{ki} and \hat{b}_i are equal in the liquid and vapor phases, all K-factors can be computed from:

$$\ln K_i = \sum_{k=1}^m h_k^\Delta \hat{s}_{ki} + h_{m+1}^\Delta \hat{b}_i + h_{m+2}^\Delta \quad , \quad (23)$$

with $h_\alpha^\Delta \equiv h_\alpha^V - h_\alpha^L$ ($\alpha = 1, \dots, m+2$). Performing the calculations in the h -space with size $m+2$ leads to another remarkable reduction in the number of variables in the multi-component flash calculation, i.e. to dimension $m+2$ instead of n regardless of the number of components in the mixture.

We note that these h -based reduced parameters are Lagrange multipliers of the classical reduced parameters, similar to the reduced parameters introduced by Nichita and Graciaa¹⁵. Hence, the reduced-space iteration has a better condition number and will converge faster than other methods²².

3.1 Thermodynamic relations for non-isothermal flashes

For non-isothermal flash calculations, it is necessary to compute additional thermodynamic quantities such as the specific molar enthalpy, internal energy, and heat capacities at constant volume and pressure. They are typically calculated as a summation of the ideal part, which is here evaluated as a function of temperature using the 9-coefficient NASA polynomials²³, and the excess part obtained from the state equation using the reduced parameters. Overall mixture quantities are computed through

$$\eta^{mix} = (1 - \theta) \eta^L + \theta \eta^V \quad , \quad (24)$$

where $\eta \in \{u, h, c_v, c_p\}$ are specific internal energy, enthalpy, and heat capacities at constant volume and pressure. The molar specific internal energy of the liquid or vapor (superscripts L and V are not repeated for brevity) is computed via

$$u = \sum_{i=1}^n z_i u_i^{ig}(T) + \frac{a - T(\partial a / \partial T)}{(\delta_2 - \delta_1)b} \ln \left(\frac{v + \delta_1 b}{v + \delta_2 b} \right), \quad (25)$$

where u_i^{ig} is the ideal gas (NASA polynomial) molar specific internal energy of pure component i ; a is obtained from Eq. (20) and its first temperature derivative is

$$\frac{\partial a}{\partial T} = 2 \sum_{k=1}^m \lambda_k q_k \frac{\partial q_k}{\partial T}, \quad (26)$$

with

$$\frac{\partial q_k}{\partial T} = -\frac{R}{2} \sqrt{\frac{\Omega_a}{T}} \sum_{i=1}^n \frac{z_i c(\omega_i) s_{ki}}{\text{sgn}(\vartheta_i)} \sqrt{\frac{T_{ci}}{p_{ci}}}, \quad (27)$$

where $\text{sgn}(\vartheta_i)$ is the sign function of variable $\vartheta_i = 1 + c(\omega_i)(1 - \sqrt{T/T_{ci}})$ and its value is equal to plus one for $\vartheta_i > 0$ and equal to minus one otherwise. The molar specific enthalpy of the mixture is defined as

$$h = u + pv, \quad (28)$$

where p is either known or computed via Eq. (2). The molar specific heat capacity at constant volume for a multi-component mixture can be computed via

$$c_v = \sum_{i=1}^n z_i c_{v,i}^{ig}(T) + \frac{T(\partial^2 a / \partial T^2)}{(\delta_1 - \delta_2)b} \ln \left(\frac{v + \delta_1 b}{v + \delta_2 b} \right). \quad (29)$$

Here, $c_{v,i}^{ig}$ is the ideal gas molar specific heat capacity at constant volume for the component i , which is computed as a function of temperature using NASA polynomials, and the second derivative $\partial^2 a / \partial T^2$ is

$$\frac{\partial^2 a}{\partial T^2} = 2 \sum_{k=1}^m \lambda_k \left[\left(\frac{\partial q_k}{\partial T} \right)^2 + q_k \frac{\partial^2 q_k}{\partial T^2} \right] \quad (30)$$

with

$$\frac{\partial^2 q_k}{\partial T^2} = \frac{R}{4T} \sqrt{\frac{\Omega_a}{T}} \sum_{i=1}^n \frac{z_i c(\omega_i) s_{ki}}{\text{sgn}(\vartheta_i)} \sqrt{\frac{T_{ci}}{p_{ci}}}. \quad (31)$$

The molar specific heat capacity at constant pressure of the mixture is computed from the thermodynamic relation

$$c_p = c_v - T \frac{(\partial p / \partial T)^2}{\partial p / \partial v}, \quad (32)$$

Algorithm 1: VT and PT flash calculations

Result: K-factors of a multi-component vapor-liquid equilibrium

Step 0: Estimate initial values of K-factors using the input values or via the Wilson's correlation in case of blind flashes;

while *convergence criteria not met* **do**

Step 1: Calculate θ by solving the Rachford-Rice equation (Eq. 14);

Step 2: Determine molar compositions x and y (Eq. 15) and then compute parameters q_k and b for both phases (Eqs. 19 and 4);

Step 3: Compute molar specific volumes v^L and v^V using pressure equality and volume constraint equations in case of VT-flash and two state equations of liquid and vapor in case of PT-flash;

Step 4: Evaluate Jacobian matrix and update the reduced principal variables for the Newton-Raphson iteration or update the principal variables via their definitions in case of the successive substitution method;

Step 5: Update K-factors (Eq. 23) and check the convergence criteria.

end

where the derivatives of pressure with respect to the specific volume and temperature are

$$\frac{\partial p}{\partial v} = -\frac{RT}{(v-b)^2} + \frac{a[2v + (\delta_1 + \delta_2)b]}{(v + \delta_1 b)^2 (v + \delta_2 b)^2} \quad (33)$$

and

$$\frac{\partial p}{\partial T} = \frac{R}{v-b} - \frac{\partial a / \partial T}{(v + \delta_1 b)(v + \delta_2 b)}. \quad (34)$$

4 Numerical algorithms

4.1 Isothermal flashes

In this section, numerical solution procedures for two important isothermal phase splitting cases, PT and VT-flashes, are presented. In Algorithm 1, we need to estimate the initial K-factors at Step 0: if there is no promising data available (blind flash), Wilson's correlation

$$K_i = \frac{p_{ci}}{p} \exp \left[5.373 (1 + \omega_i) \left(1 - \frac{T_{ci}}{T} \right) \right], \text{ for } i = 1 \dots n \quad (35)$$

is commonly employed for the initialization of the iteration. This is straightforward if the pressure and temperature are known as in the PT-flash; in the case of a blind VT-flash, however, the pressure is unknown. In this case, one could estimate the pressure from the state equation of the mixture by using the total specific volume \hat{v} , temperature T , and overall mole fractions \hat{z}_i as an input, but

this will result in negative pressures in many cases. A simple remedy is to set a minimum value in pressure estimation¹⁹, or to employ the initialization method based on the vapor pressures of the components^{24,25}. We propose to use the geometric average of the pressures of the dew and bubble points estimated as

$$p \approx \sqrt{\sum_{i=1}^n \hat{z}_i p_i^{sat} / \sum_{i=1}^n \frac{\hat{z}_i}{p_i^{sat}}}, \quad (36)$$

where p_i^{sat} is the vapor pressure of the pure component i , which can be estimated from Raoult's law and Wilson's correlation.

In Step 1, we need to solve the Rachford-Rice Eq. (14) to determine the vapor mole fraction. Usually, a Newton method is coupled with a bisection method for reasons explained by Michelsen and Mollerup²¹. In order to preserve the fully quadratic convergence rate of the Newton method, we rather use the convex transformation technique of Nichita and Leibovici²⁶. In the convex transformation technique, the first and last index are assigned to the components with maximum and minimum K-factors, and vectors $c_i = 1/(1 - K_i)$ and $d_i = (c_1 - c_i)/(c_n - c_1)$ are obtained for all components. Two convex functions of the variable $\sigma = (\theta - c_1)/(c_n - \theta)$, can be then computed:

$$G(\sigma) = (1 + \sigma)S(\sigma), \quad (37a)$$

$$H(\sigma) = -\sigma(1 + \sigma)S(\sigma), \quad (37b)$$

where

$$S(\sigma) = \sum_{i=1}^n \frac{z_i}{d_i + \sigma(1 + d_i)}. \quad (38)$$

For any starting value σ_0 in the range of $(0, +\infty)$, monotonic convergence of the Newton iteration is guaranteed for one of these two functions. The estimated value of σ is updated via

$$\sigma_{new} = \begin{cases} \sigma - G(\sigma)/G'(\sigma) & , \text{for } G(\sigma) > 0 \\ \sigma - H(\sigma)/H'(\sigma) & , \text{for } G(\sigma) < 0 \end{cases} \quad (39)$$

where G' and H' are derivatives of G and H with respect to σ :

$$G'(\sigma) = S(\sigma) + (1 + \sigma)S'(\sigma), \quad (40a)$$

$$H'(\sigma) = -(1 + 2\sigma)S(\sigma) - \sigma(1 + \sigma)S'(\sigma), \quad (40b)$$

and

$$S'(\sigma) = \sum_{i=1}^n \frac{-z_i(1+d_i)}{(d_i + \sigma(1+d_i))^2} . \quad (41)$$

The Newton iteration is repeated with σ_{new} until the convergence criteria is met. The vapor mole fraction is then obtained via $\theta = (c_1 + \sigma c_n)/(1 + \sigma)$.

In Step 2, molar compositions of the liquid x_i and vapor y_i for ($i = 1 \dots n$) are computed using Eq. (15). Then m reduced parameters q_k and mixture co-volume parameter b are obtained using Eqs. (19) and (4) for both phases.

In Step 3, the energy parameter a is computed for the liquid and vapor phases using their m reduced parameters via Eq. (20). For the case of PT-flash, in which the value of the equilibrium pressure p is given, the specific volume is then computed for the vapor and liquid phases separately. For general cubic EoS Eq. (2) this means to find the roots of the cubic equation that is written below for the liquid phase:

$$v_L^3 + \varrho_2 v_L^2 + \varrho_1 v_L + \varrho_0 = 0 , \quad (42)$$

where

$$\begin{aligned} \varrho_0 &= -a_L b_L / p - (b_L + RT/p) \delta_1 \delta_2 b_L^2 , \\ \varrho_1 &= \delta_1 \delta_2 b_L^2 + a_L / p - (\delta_1 + \delta_2) b_L (b_L + RT/p) , \\ \varrho_2 &= (\delta_1 + \delta_2 - 1) b_L - RT/p . \end{aligned} \quad (43)$$

The same equation is holds for the vapor phase. We use Cardano's algorithm to determine all roots of Eq. (42). If more than one real root is found, the root associated with the lowest Gibbs free energy is selected²¹.

For the VT-flash, in which the value of the total molar specific volume \hat{v} is given, we first compute the molar specific volume of one phase from the volume constraint $(1 - \theta)v_L + \theta v_V = \hat{v}$ and then substitute it into the pressure equality equation. The resulting equation is a quintic function of the other phase specific volume that is given below for the liquid phase:

$$\varsigma_5 v_L^5 + \varsigma_4 v_L^4 + \varsigma_3 v_L^3 + \varsigma_2 v_L^2 + \varsigma_1 v_L + \varsigma_0 = 0 \quad (44)$$

where

$$\begin{aligned}
\varsigma_0 &= (\alpha_2^L \alpha_5^V - \alpha_2^V \alpha_5^L) \theta^3 - (\alpha_5^L \alpha_1^V - \alpha_4^V \alpha_2^L) \hat{v} \theta^2 + (\alpha_2^L \alpha_3^V - \alpha_5^L) \theta \hat{v}^2 + \alpha_2^L \hat{v}^3 , \\
\varsigma_1 &= (\alpha_1^L \alpha_5^V - \alpha_5^L \alpha_1^V + \alpha_4^V \alpha_2^L - \alpha_2^V \alpha_4^L) \theta^3 + (\alpha_1^L \alpha_3^V + 3\alpha_2^L - \alpha_4^L) \hat{v}^2 \theta + (\hat{v} \alpha_1^L - 3\alpha_2^L) \hat{v}^2 \\
&\quad + 2(\alpha_5^L - \alpha_2^L \alpha_3^V) \hat{v} \theta + (\alpha_1^L \alpha_4^V - \alpha_1^V \alpha_4^L + 2\alpha_2^L \alpha_3^V - 2\alpha_5^L) \hat{v} \theta^2 + (\alpha_5^L \alpha_1^V - \alpha_4^V \alpha_2^L) \theta^2 , \\
\varsigma_2 &= (\alpha_1^L \alpha_4^V - \alpha_1^V \alpha_4^L + \alpha_2^L \alpha_3^V - \alpha_2^V \alpha_3^L - \alpha_5^L + \alpha_5^V) \theta^3 + (\hat{v}^2 - 3\hat{v} \alpha_1^L + 3\alpha_2^L) \hat{v} \\
&\quad + (2\alpha_1^L \alpha_3^V - \alpha_1^V \alpha_3^L + 3\alpha_2^L - 2\alpha_4^L + \alpha_4^V) \hat{v} \theta^2 + (\alpha_1^V \alpha_4^L - \alpha_1^L \alpha_4^V - 2\alpha_2^L \alpha_3^V + 2\alpha_5^L) \theta^2 \\
&\quad + (3\alpha_1^L - \alpha_3^L + \alpha_3^V) \hat{v}^2 \theta + 2(\alpha_4^L - \alpha_1^L \alpha_3^V - 3\alpha_2^L) \hat{v} \theta + (\alpha_2^L \alpha_3^V - \alpha_5^L) \theta , \\
\varsigma_3 &= (\alpha_1^L \alpha_3^V - \alpha_1^V \alpha_3^L + \alpha_2^L - \alpha_2^V - \alpha_4^L + \alpha_4^V) \theta^3 + (3\alpha_1^L - \alpha_1^V - 2\alpha_3^L + 2\alpha_3^V) \hat{v} \theta^2 \\
&\quad + (\alpha_1^V \alpha_3^L - 2\alpha_1^L \alpha_3^V - \alpha_4^V - 3\alpha_2^L + 2\alpha_4^L) \theta^2 + (-6\alpha_1^L + 2\alpha_3^L - 2\alpha_3^V) \hat{v} \theta \\
&\quad + (2\hat{v}^2 + \alpha_1^L \alpha_3^V + 3\alpha_2^L - \alpha_4^L) \theta - 3\hat{v}^2 + 3\hat{v} \alpha_1^L - \alpha_2^L , \\
\varsigma_4 &= [(\alpha_1^L - \alpha_1^V - \alpha_3^L + \alpha_3^V) \theta^2 + (\hat{v} - 2\alpha_1^L + \alpha_3^L - \alpha_3^V) \theta - 3\hat{v} + \alpha_1^L] (\theta - 1) , \\
\varsigma_5 &= -(\theta - 1)^2 .
\end{aligned} \tag{45}$$

Here, parameters $\alpha_i (i = 1 \dots 5)$ are computed via the following expressions using the liquid and vapor co-volume and energy parameters:

$$\begin{aligned}
\alpha_1 &= b(\delta_1 + \delta_2) - a/RT , \\
\alpha_2 &= b(b\delta_1\delta_2 + a/RT) , \\
\alpha_3 &= b(\delta_1\delta_2 - 1) , \\
\alpha_4 &= b^2(\delta_1 + \delta_2 - \delta_1\delta_2) , \\
\alpha_5 &= -b^3\delta_1\delta_2 .
\end{aligned} \tag{46}$$

Since there is no analytical solution, Eq. (44) has to be solved by iterative methods to obtain v_L . We use a Newton method with a starting point very close to the co-volume of the mixture in this study. Afterwards, the vapor's specific volume is obtained through the volume constraint $v_V = [\hat{v} - (1 - \theta)v_L] / \theta$.

In Step 4, we update the principal variables via their definitions in the first iteration (corresponding to a successive substitution iteration (SSI)) or evaluate Jacobian matrix and update the reduced principal variables for the Newton-Raphson iteration (NRI). In the case of the SSI, the new values of the reduced principal variables are obtained as the difference between the h values of the vapor

and liquid phase calculated via Eq. (22). In the case of the NRI, first the error functions

$$e_\alpha = h_\alpha^V - h_\alpha^L - h_\alpha^\Delta, \text{ for } \alpha = 1 \dots m + 2 \quad (47)$$

and the associated Jacobian matrix

$$J_{\alpha\beta} = \frac{\partial e_\alpha}{\partial h_\beta^\Delta} = \frac{\partial h_\alpha^V}{\partial h_\beta^\Delta} - \frac{\partial h_\alpha^L}{\partial h_\beta^\Delta} - \delta_{\alpha\beta}, \text{ for } \alpha, \beta = 1 \dots m + 2 \quad (48)$$

are calculated, in which $\delta_{\alpha\beta}$ is the Kronecker delta function. Next, the resulting set of linear equations $J\Delta\vec{h}^\Delta = \vec{e}$, can be solved by using the Gauss elimination method with partial pivoting to compute $\Delta\vec{h}^\Delta = \vec{h}_{new}^\Delta - \vec{h}_{old}^\Delta$ and the new values of the reduced principal variables

$$\vec{h}_{new}^\Delta = \vec{h}_{old}^\Delta + \Delta\vec{h}^\Delta. \quad (49)$$

In order to find the analytical expressions of the entries of the Jacobian matrix (48), we used the classical $m + 2$ reduced parameters including $q_k (k = 1 \dots m)$, b , and θ as the helping variables in the derivative chain rule for the required partial derivatives

$$\frac{\partial h_\alpha^j}{\partial h_\beta^\Delta} = \sum_{k=1}^m \left(\frac{\partial h_\alpha^j}{\partial q_k^j} + \frac{\partial h_\alpha^j}{\partial v^j} \frac{\partial v^j}{\partial q_k^j} \right) \frac{\partial q_k^j}{\partial h_\beta^\Delta} + \left(\frac{\partial h_\alpha^j}{\partial b^j} + \frac{\partial h_\alpha^j}{\partial v^j} \frac{\partial v^j}{\partial b^j} \right) \frac{\partial b^j}{\partial h_\beta^\Delta} + \frac{\partial h_\alpha^j}{\partial v^j} \frac{\partial v^j}{\partial \theta} \frac{\partial \theta}{\partial h_\beta^\Delta}, \text{ for } j = L, V. \quad (50)$$

The required partial derivatives of the coefficients h are obtained via Eq. (22). The derivatives with respect to the reduced variable q_k are

$$\begin{aligned} \partial h_\alpha / \partial q_k &= 2\delta_{\alpha k} \lambda_k q_k \ln[(v + \delta_1 b) / (v + \delta_2 b)] / [(\delta_1 - \delta_2) b R T], \text{ for } \alpha = 1 \dots m \\ \partial h_{m+1} / \partial q_k &= 2\lambda_k q_k \left\{ \begin{array}{l} v b / [(v + \delta_1 b)(v + \delta_2 b)] - \\ \ln [(v + \delta_1 b) / (v + \delta_2 b)] / (\delta_1 - \delta_2) \end{array} \right\} / (R T b^2), \\ \partial h_{m+2} / \partial q_k &= 0. \end{aligned} \quad (51)$$

In addition, the derivatives with respect to the co-volume of the phase are

$$\begin{aligned}
\partial h_\alpha / \partial b &= 2\lambda_\alpha q_\alpha \left\{ \frac{vb / [(v + \delta_1 b)(v + \delta_2 b)] - \ln [(v + \delta_1 b)/(v + \delta_2 b)] / (\delta_1 - \delta_2)}{RTb^2} \right\}, \text{ for } \alpha = 1 \dots m \\
\partial h_{m+1} / \partial b &= av \left\{ \frac{2 \ln [(v + \delta_1 b)/(v + \delta_2 b)] / [bv(\delta_1 - \delta_2)] - [4\delta_1\delta_2 b^2 + 3vb(\delta_1 + \delta_2) + 2v^2] / [(v + \delta_1 b)(v + \delta_2 b)]^2}{RTb^2} \right\} - 1/(v - b), \\
\partial h_{m+2} / \partial b &= -1/(v - b),
\end{aligned} \tag{52}$$

where a is computed via Eq. (20) as a function of reduced parameters. The derivatives respect to the specific volume of the phase are

$$\begin{aligned}
\partial h_\alpha / \partial v &= -2\lambda_\alpha q_\alpha / [RT(v + \delta_1 b)(v + \delta_2 b)], \text{ for } \alpha = 1 \dots m \\
\partial h_{m+1} / \partial v &= a[2b\delta_1\delta_2 + v(\delta_1 + \delta_2)] / [RT(v + \delta_1 b)^2(v + \delta_2 b)^2] + 1/(v - b), \\
\partial h_{m+2} / \partial v &= 1/(v - b).
\end{aligned} \tag{53}$$

Next, the partial derivatives of the specific volume in Eq. (50) are obtained through the implicit function theorem. For PT-flashes, we directly utilize the general cubic EoS (2) for each phase as follows:

$$\partial v^j / \partial q_k^j = -(\partial p / \partial q_k)^j / (\partial p / \partial v)^j, \text{ for } j = L, V \tag{54}$$

with $\partial p / \partial v$ from Eq. (33). By using the relationship between the a and q_k , we can compute $\partial p / \partial q_k$ as

$$\partial p / \partial q_k = -2\lambda_k q_k / [(v + \delta_1 b)(v + \delta_2 b)]. \tag{55}$$

Moreover, the derivatives with respect to the co-volume of the mixture are

$$\partial v^j / \partial b^j = -(\partial p / \partial b)^j / (\partial p / \partial v)^j, \text{ for } j = L, V \tag{56}$$

with

$$\partial p / \partial b = RT/(v - b)^2 + a[2\delta_1\delta_2 b + v(\delta_1 + \delta_2)] / [(v + \delta_1 b)(v + \delta_2 b)]^2. \tag{57}$$

It is obvious that, in PT-flashes, the partial derivatives of the specific volumes with respect to the vapor mole fraction are zero, i.e.

$$\partial v^j / \partial \theta = 0, \text{ for } j = L, V. \tag{58}$$

For utilizing the implicit function theorem for the VT-flashes, we define the function $f \equiv p^L - p^V$ and then compute the required derivatives as

$$\partial v^j / \partial q_k^j = -(\partial f / \partial q_k^j) / (\partial f / \partial v^j) \quad , \text{ for } j = L, V , \quad (59)$$

$$\partial v^j / \partial b^j = -(\partial f / \partial b^j) / (\partial f / \partial v^j) \quad , \text{ for } j = L, V , \quad (60)$$

where partial derivatives of f can be computed using the chain rule. For instance, when $j = L$, we obtain

$$\partial f / \partial v^L = (\partial p / \partial v)^L - (\partial p / \partial v)^V (\partial v^V / \partial v^L) , \quad (61)$$

$$\partial f / \partial q_k^L = (\partial p / \partial q_k)^L - (\partial p / \partial q_k)^V (\partial q_k^V / \partial q_k^L) , \quad (62)$$

$$\partial f / \partial b^L = (\partial p / \partial b)^L - (\partial p / \partial b)^V (\partial b^V / \partial b^L) , \quad (63)$$

along with $\partial v^V / \partial v^L = \partial q_k^V / \partial q_k^L = \partial b^V / \partial b^L = (\theta - 1) / \theta$. Subsequently, the partial derivatives of specific volumes respect to the vapor mole fraction are computed through

$$\partial v^j / \partial \theta = -(\partial f / \partial \theta)^j / (\partial f / \partial v^j) \quad , \text{ for } j = L, V , \quad (64)$$

where $\partial f / \partial \theta$ for the liquid and vapor phases are

$$(\partial f / \partial \theta)^L = \left[\sum_{k=1}^m (q_k^L - q_k^V) (\partial f / \partial q_k^V) + (b^L - b^V) (\partial f / \partial b^V) + (v^L - v^V) (\partial f / \partial v^V) \right] / \theta , \quad (65)$$

$$(\partial f / \partial \theta)^V = \left[\sum_{k=1}^m (q_k^V - q_k^L) (\partial f / \partial q_k^L) + (b^V - b^L) (\partial f / \partial b^L) + (v^V - v^L) (\partial f / \partial v^L) \right] / (1 - \theta) . \quad (66)$$

Finally, partial derivatives of the reduced parameters $q_k (k = 1 \dots m)$ as well as b with respect to principal variables $h_\beta^\Delta (\beta = 1 \dots m + 2)$ can be obtained via their definitions: for all m reduced parameters

$$\partial q_k / \partial h_\beta^\Delta = \sum_{i=1}^n (\partial z_i / \partial h_\beta^\Delta) \hat{s}_{ki} , \quad (67)$$

and for the co-volume parameter

$$\partial b / \partial h_\beta^\Delta = \sum_{i=1}^n (\partial z_i / \partial h_\beta^\Delta) \hat{b}_i . \quad (68)$$

In both equations, we need the derivatives of the phase mole fractions z_i , which is equal to x_i and y_i for liquid and vapor phases, with respect to the principal variables. Using the Rachford-Rice

equation and the definition of the equilibrium ratio, we obtain

$$\partial x_i / \partial h_\beta^\Delta = d_i [\theta \partial K_i / \partial h_\beta^\Delta + (K_i - 1) \partial \theta / \partial h_\beta^\Delta] , \quad (69)$$

and

$$\partial y_i / \partial h_\beta^\Delta = d_i [(1 - \theta) \partial K_i / \partial h_\beta^\Delta + K_i (K_i - 1) \partial \theta / \partial h_\beta^\Delta] , \quad (70)$$

where $d_i = -z_i / [1 + \theta(K_i - 1)]^2$. The partial derivative with respect to principal variables is expressed as follows for all K-values:

$$\begin{aligned} \partial K_i / \partial h_\beta^\Delta &= K_i \hat{s}_{\beta i} , \text{ for } \beta = 1 \dots m \\ \partial K_i / \partial h_{m+1}^\Delta &= K_i \hat{b}_i , \\ \partial K_i / \partial h_{m+2}^\Delta &= K_i , \end{aligned} \quad (71)$$

and for the vapor mole fraction and the index the index in the range from $\beta = 1$ to $m + 2$:

$$\partial \theta / \partial h_\beta^\Delta = \sum_{i=1}^n d_i (\partial K_i / \partial h_\beta^\Delta) / \sum_{i=1}^n d_i (K_i - 1)^2 . \quad (72)$$

In Step 5, the logarithm of equilibrium ratios are computed from the updated principal variables via Eq. 23 and the following convergence criterion is checked:

$$\| \ln K_i^{new} - \ln K_i^{old} \| \leq \varepsilon_k . \quad (73)$$

We propose and use $\varepsilon_k = 10^{-2}$ for the initial SSI and $\varepsilon_k = 10^{-10}$ for NRI, but one SSI step is usually enough for the most of cases. If the solution is not converged, we jump back to step 1 with the new K-values.

4.2 Non-isothermal flashes

In this section, the numerical solution method for the HP- and UV-flashes are explained. The main idea is to use the most appropriate isothermal flash (that is, PT for HP and VT for UV) and iterate its input temperature in such a way that the specific internal energy (UV) or enthalpy (HP) converge to the given value. The numerical procedure is summarized in Algorithm 2 and explained in more detailed in the following:

In Step 0, the temperature of the mixture is estimated. To provide an initial guess at regions close

Algorithm 2: UV and HP flash calculations

Result: Equilibrium temperature

Step 0: Estimate the initial value of temperature;

while *convergence criteria not met* **do**

Step 1: Execute one VT-flash or PT-flash according to the availability of the specific volume or pressure and the latest available temperature;

Step 2: In case of UV-flash, compute the specific internal energy and c_v of the mixture, or in case of HP-flash, compute the specific enthalpy and c_p of the mixture;

Step 3: Update the temperature and check the convergence criteria;

end

to the critical point or near phase boundaries, one can estimate the temperature by considering the mixture as single-phase and then iterate the EoS for the given specific internal energy or enthalpy.

In Step 1, we perform an isothermal flash calculation using the method that most closely corresponds to the targeted non-isothermal problem, that is, we perform a PT-flash in the case of the HP problem and a VT-flash for the case of the UV-flash. It is clear that for the first iteration these iso-thermal flashes require an estimate of the K-factors (it might exist from previous data otherwise those can be estimated via Wilson's correlation as discussed above) whereas for the subsequent iterations, the previously computed values of K-factors can be used to accelerate computations.

In Step 2, the internal energy of the mixture u^{mix} and its derivatives with respect to the temperature, i.e. c_v^{mix} , for the case of UV-flash and the specific enthalpy of the mixture h^{mix} and its derivative with respect to the temperature, i.e. c_p^{mix} , for the case of HP-flash are computed. All derivatives are computed from the reduced variables as explained in Section 3.1.

In Step 3, the estimated temperature is updated by a Newton iteration with line search \mathcal{L} in the range of $[0, 1]$ for the case of UV-flashes:

$$T^{new} = T - \mathcal{L}(\hat{u} - u^{mix})/c_v^{mix} \quad (74)$$

and for the case of HP-flashes:

$$T^{new} = T - \mathcal{L}(\hat{h} - h^{mix})/c_p^{mix} \quad (75)$$

Using the line search \mathcal{L} ensures global convergence of the algorithm and renders the temperature initial guess less important. Subsequently, the relative error is computed, i.e. $\varepsilon_r = |(\hat{h} - h^{mix})/\hat{h}|$ or $\varepsilon_r = |(\hat{u} - u^{mix})/\hat{u}|$ for HP or UV-flashes, respectively. Steps 1 to 3 are repeated until the

Table 1: Critical properties and acentric factors of components used in this study.

Name	T_c [K]	p_c [bar]	ω [-]	Name	T_c [K]	p_c [bar]	ω [-]
C ₁	190.6	45.4	0.008	nC ₆	507.5	30.1	0.305
C ₂	305.4	48.2	0.098	nC ₇	540.3	27.4	0.305
C ₃	369.8	41.9	0.152	nC ₈	568.8	24.9	0.396
nC ₄	425.2	37.5	0.193	nC ₁₀	617.9	21.0	0.484
nC ₅	469.6	33.3	0.251	nC ₁₄	691.9	15.2	0.747

Table 2: Total mixture properties of the test fluids.

Properties [unit]	Y8 mixture			MY10 mixture		
	Point A	Point B	Point C	Point D	Point E	Point F
Temperature [K]	295.40000	335.20000	375.30000	509.10000	566.60000	563.50000
Pressure [bar]	198.10000	134.50000	194.80000	104.90000	75.400000	32.700000
Volume [L/mol]	0.0805680	0.1533446	0.1273056	0.2280903	0.3846589	1.0596464
Enthalpy [KJ/mol]	-94.704181	-90.636841	-87.895981	-142.74142	-124.94053	-120.73426
Int. Energy [KJ/mol]	-96.300235	-92.699326	-90.375895	-145.13409	-127.84086	-124.19930

Table 3: Molar composition of vapor and liquid in equilibrium at the states selected for the detailed analysis of the convergence of the flash algorithms.

Y8	Point A		Point B		Point C	
	Liquid	Vapor	Liquid	Vapor	Liquid	Vapor
C ₁	0.74744792	0.84906008	0.47658529	0.87746005	0.60400388	0.81762325
C ₂	0.06057858	0.05408446	0.06296756	0.05530475	0.05844115	0.05652908
C ₃	0.03589832	0.02725004	0.05092726	0.02646516	0.03965730	0.03025112
nC ₅	0.06266242	0.03497518	0.13974651	0.02656967	0.09067889	0.04396745
nC ₇	0.05032462	0.02204618	0.13898012	0.01144221	0.09260111	0.03070421
nC ₁₀	0.04308814	0.01258406	0.13079327	0.00275817	0.11461768	0.02092489
MY10	Point D		Point E		Point F	
	Liquid	Vapor	Liquid	Vapor	Liquid	Vapor
C ₁	0.32277170	0.65714256	0.27245022	0.42483512	0.07783597	0.38155198
C ₂	0.02889804	0.04243037	0.02539431	0.03444446	0.00953245	0.03237280
C ₃	0.03944780	0.04622895	0.03581565	0.04403788	0.01633421	0.04274357
nC ₄	0.06033169	0.05625849	0.05673424	0.06315144	0.03147630	0.06330675
nC ₅	0.04080501	0.03091922	0.03964769	0.04033998	0.02627885	0.04159069
nC ₆	0.03095915	0.01918057	0.03106314	0.02897407	0.02441470	0.03064750
nC ₇	0.05206707	0.02668295	0.05397352	0.04616557	0.05015849	0.04998163
nC ₈	0.05247517	0.02207942	0.05603950	0.04417191	0.06088237	0.04873841
nC ₁₀	0.31843114	0.09209178	0.36069877	0.24142602	0.52938744	0.27340711
nC ₁₄	0.05381324	0.00698568	0.06818296	0.03245354	0.17369922	0.03565955

convergence criterion is satisfied, for the calculations presented in this paper until $\varepsilon_r < 10^{-10}$.

5 Numerical results

We have developed a Fortran implementation of the proposed flash algorithms for the four discussed isothermal and non-isothermal flash calculations, and tested it for a large number of different multi-component mixtures and different cubic EoS. The selected representative cases that we will present discuss in the following use the PR EoS and the values for the critical temperatures, critical pressures and acentric factors that are listed in Table 1.

5.1 Convergence behavior and robustness

Two mixtures with specified compositions including a synthetic condensate gas and synthetic oil are selected in order to validate and evaluate the performance of proposed flash algorithms. The first fluid is the Y8 mixture introduced by Yarborough²⁷. It is a six-component synthetic gas condensate of normal alkanes including 80.97 C₁, 5.66 C₂, 3.06 C₃, 4.57 nC₅, 3.30 nC₇, and 2.44 nC₁₀ mole percents with a zero binary interaction matrix. With our reduction method, the latter results in only three governing equations for the reduced variables. The second fluid is the MY10 mixture introduced by Metcalfe and Yarborough²⁸. It is a ten-component mixture with overall molar fractions of 0.35 C₁, 0.03 C₂, 0.04 C₃, 0.06 nC₄, 0.04 nC₅, 0.03 nC₆, 0.05 nC₇, 0.05 nC₈, 0.30 nC₁₀, and 0.05 nC₁₄. For this mixture, all binary interaction coefficients are zero except those between the methane and the other components as reported by Firoozabadi and Pan²⁹. This sparse binary interaction matrix results in three non-zero eigenvalues $\lambda_1 = 9.9574$, $\lambda_2 = 0.0707$ and $\lambda_3 = -0.0280$.

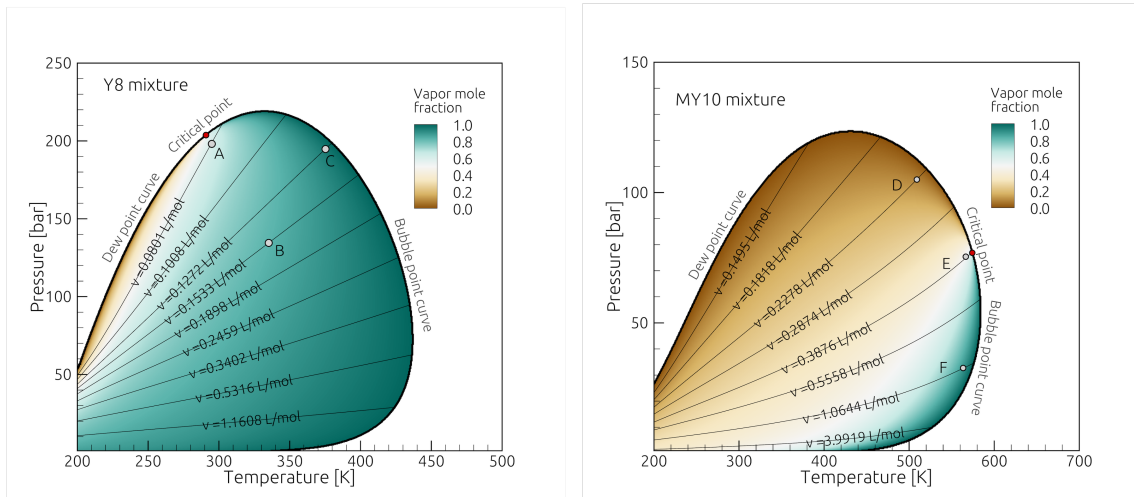


Figure 1: Phase diagrams for the Y8 and MY10 mixtures including isochores and the states selected for the detailed analysis of the convergence of the flash algorithms.

In Fig. 1, the phase diagrams for the two mixtures with contours of vapor mole fractions are shown. These diagrams are generated without any convergence problems of the blind PT-flashes over a fine Cartesian grid with 800×800 nodes for the pressure - temperature range shown in the figure. This very fine grid is selected in order to check the applicability of the PT-flash algorithm at many different conditions very quite close to the phase boundaries and the critical point, where other methods may converge either very slowly or not at all.

Next, VT-flashes have been conducted along isochores drawn on the phase diagram. Selected isochoric lines are drawn in Fig. 1 to show the pressure evolution during constant volume heating

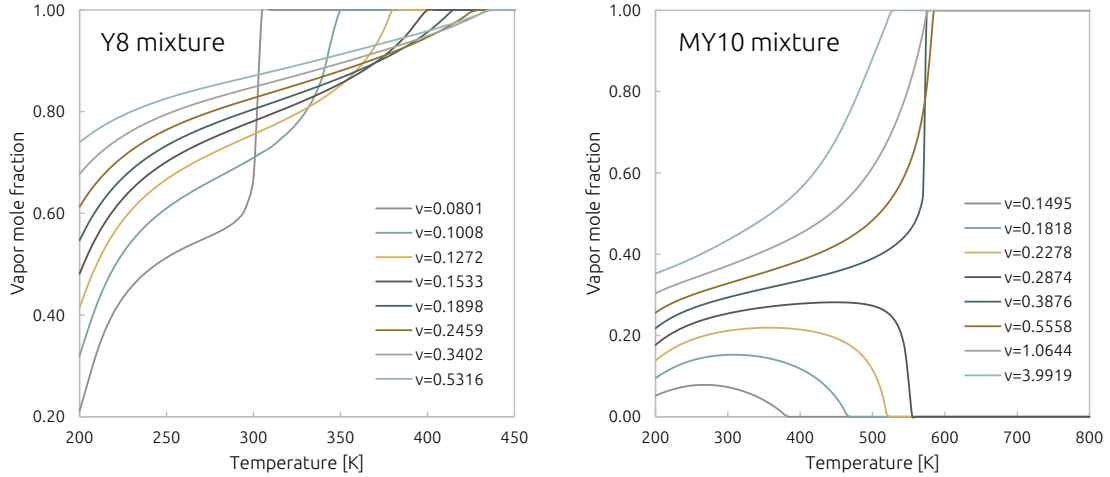


Figure 2: Vapor mole fraction curves as a function of temperature generated by the VT-flash algorithm corresponding to the lines shown in Fig. 1.

or cooling of a typical condensate gas or synthetic oil. The corresponding vapor mole fraction curves shown in Fig. 2 were computed using the proposed VT-flash algorithm with the starting temperature of 200 [K] and a step size of 1 [K] up-to the saturation point. The retrograde behavior of MY10 for specific volumes lower than or equal to 0.2874 [L/mol] is an interesting phenomena: by increasing the temperature from 200 [K] the vapor mole fraction first increases with temperature and then decreases to zero. We verified that the results agree with our previous implementation of Michelson’s methods³ and that the results of the VT-flashes are the same as those obtained with the PT-flashes up to machine round-off precision.

The performance of the isothermal and non-isothermal flash algorithms is investigated for six algorithmically challenging points (A-F) marked in the phase diagrams of the mixtures, see Fig. 1. The overall thermodynamic properties at these points are listed in Table 2 and results for the molar composition of the vapor and liquid in equilibrium are shown in Table 3. These values are equal for all types of flash calculations.

The evolution of the Euclidean residual norm for the PT-flash calculations at points A (198.1 [bar], 295.4 [K]), B (134.5 [bar], 335.2 [K]), and C (194.8 [bar], 375.3 [K]) for the Y8 mixture, and at points D (104.9 [bar], 509.1 [K]), E (75.4 [bar], 566.6 [K]), and F (32.7 [bar], 566.6 [K]) for the MY10 mixture are plotted in Fig. 3. For all points, one SSI has been carried out on the initial K-factors obtained from Wilson’s correlation before switching to the NRI. Results indicate that PT-flash algorithm requires about 6 – 8 iterations for the points at the heart of the two-phase dome, near the phase boundaries, and close to the critical point.

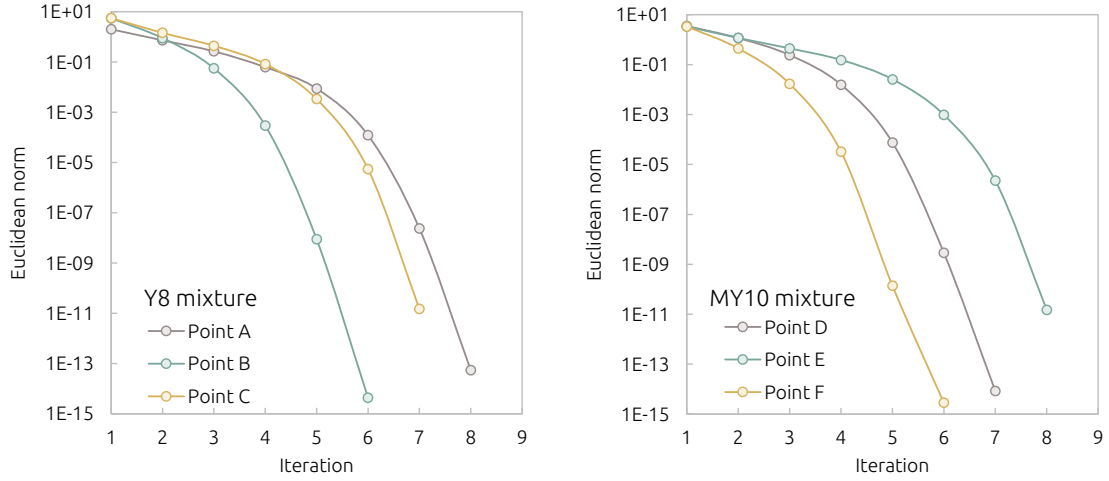


Figure 3: PT-flash convergence for the Y8 and MY10 mixtures at the points marked in Fig. 1.

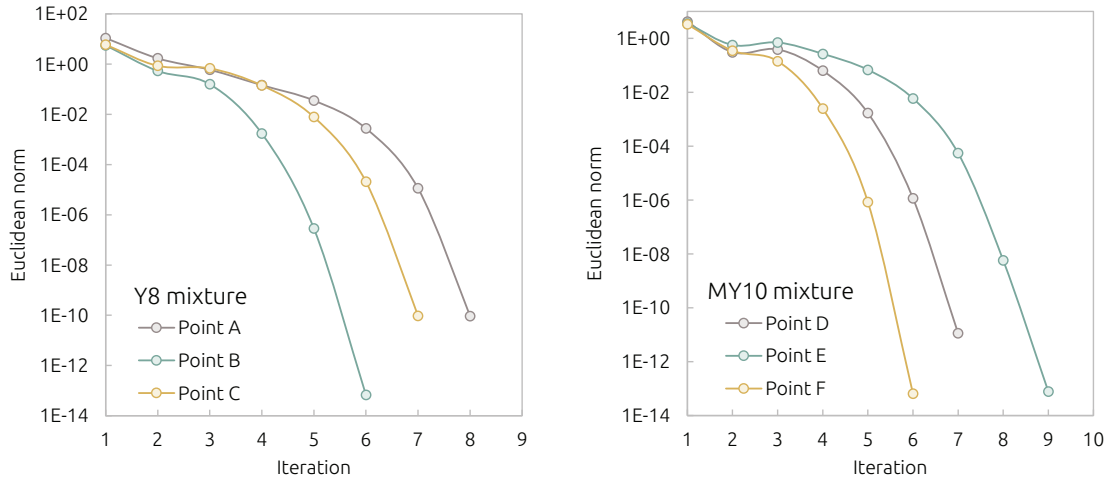


Figure 4: VT-flash convergence for the Y8 and MY10 mixtures at the points marked in Fig. 1.

The convergence of the residuals of VT-flash calculations are shown in Fig. 4 for the points A (0.0806 [L/mol], 295.4 [K]), B (0.1533 [L/mol], 335.2 [K]), and C (0.1273 [L/mol], 375.3 [K]) corresponding to the marked points on the phase diagram of the Y8 mixture, and for the points D (0.2281 [L/mol], 509.1 [K]), E (0.3847 [L/mol], 566.6 [K]), and F (1.0596 [L/mol], 563.5 [K]) corresponding to the tagged points on the phase diagram of the MY10 mixture. Initial values for the K-factors were obtained from Wilson's correlation using a pressure obtained from the state equation by the overall composition and given temperature and volumes, i.e. $p = \{188.8, 119.3, 193.2, 95.5, 74.1, 33.2\}$ [bar] for points { A to F }. As for the PT-flashes, one initial SSI was executed before switching to NRI. The VT-flash results show the same excellent convergence behavior as observed for the PT-flashes, that is, both algorithms have optimum quadratic convergence and require only very few

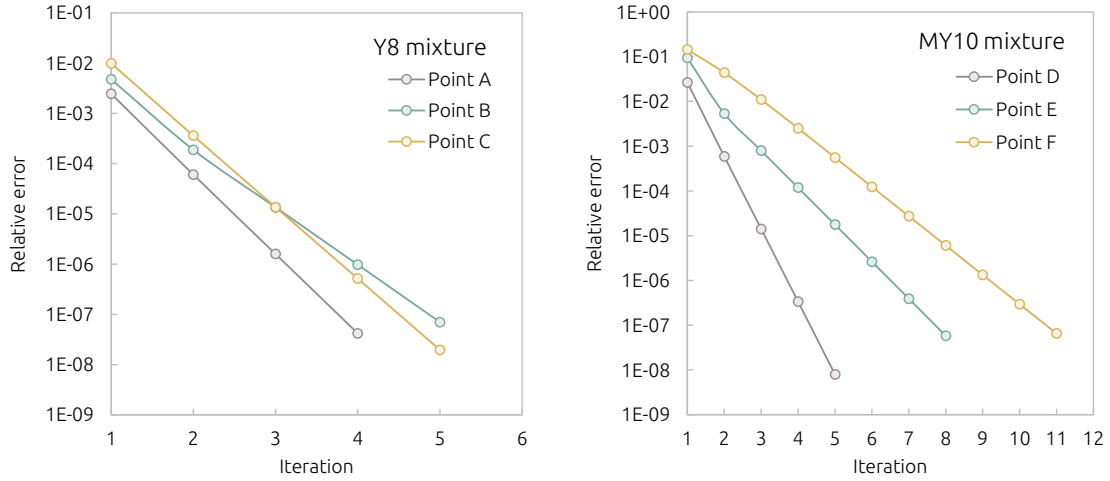


Figure 5: HP-flash convergence for the Y8 and MY10 mixtures at the points marked in Fig. 1.

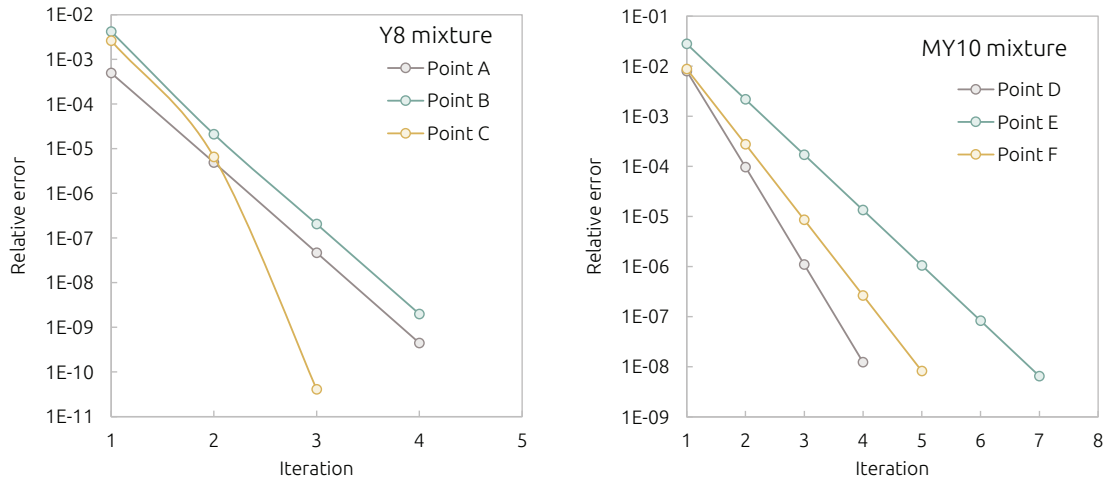


Figure 6: UV-flash convergence for the Y8 and MY10 mixtures at the points marked in Fig. 1.

iterations, with only two iterations difference between points close to and far from the extreme conditions.

Figure 5 shows the convergence of the relative errors for the blind HP-flash at points A (-94.704 [kJ/mol], 198.1 [bar]), B (-90.637 [kJ/mol], 134.5 [bar]), and C (-87.896 [kJ/mol], 194.8 [bar]) for the the condensate gas and at points D (-142.741 [kJ/mol], 104.9 [bar]), E (-124.941 [kJ/mol], 75.4 [bar]), and F (-120.734 [kJ/mol], 32.7 [bar]) for the synthetic oil. We initialize the iteration with a temperature of 250 [K] for Y8 and 400 [K] for MY10, far away from the true solution, in order to test the robustness of the non-isothermal flashes at extreme conditions. As the convergence plots show, they rapidly converge within very few iterations even with a poor initial temperature guess.

Figure 6 shows results for the blind UV-flash at the points A (-96.300 [kJ/mol], 0.0805 [L/mol]),

B (-92.699 [kJ/mol], 0.1533 [L/mol]), and C (-90.376 [kJ/mol], 0.1273 [L/mol]) for Y8 and at the points D (-145.134 [kJ/mol], 0.2281 [L/mol]), E (-127.841 [kJ/mol], 0.3847 [L/mol]), and F (-124.199 [kJ/mol], 1.0596 [L/mol]) for the MY10 mixture. As before, the initial temperature guess is 250 [K] for the Y8 gas condensate and 400 [K] for the MY10 oil mixture. The initial values for the pressure are the same as used for the VT-flash at these points, see above. We observe rapid convergence within 4 to 7 iterations to within a relative error of 10^{-8} . For the most of engineering applications, it is, however, not necessary to know the temperature with such a high precision and a much larger error, say 0.1 [K] can be tolerated. The algorithms for both non-isothermal flashes yield temperature differences of less than 0.1 [K] in just 3 iterations.

5.2 Computational time

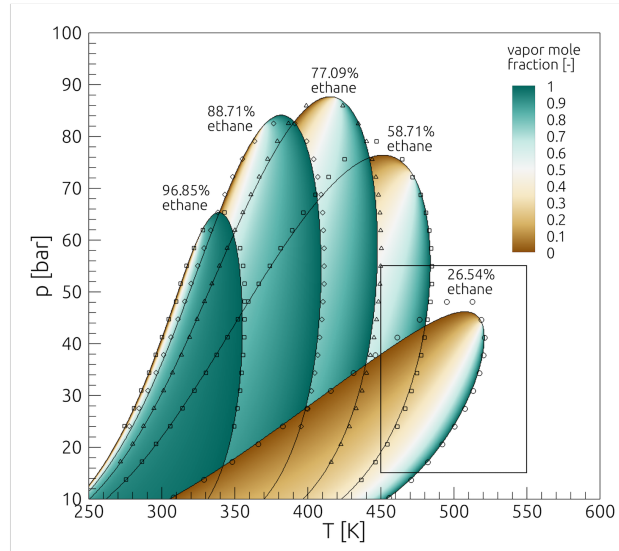


Figure 7: Phase diagram of binary mixtures of n-heptane and ethane at various molar compositions computed by the proposed algorithm. The symbols denote experimental reference data for the dew-point and bubble-point lines^{30,31}. The black box encloses the pressure-temperature domain that was used for measuring the computational performance of the flash algorithms.

In this section, we analyse the computational performance of the proposed flash algorithms for different mixtures and demonstrate the improved efficiency resulting from using a reduction method and direct VT-flashes instead of PT-flashes in the inner iteration loop of UV-flashes. For a fair quantitative evaluation, the computational time required for the new flash algorithms that we propose in this paper is compared with the highly optimized implementation of a conventional method that was developed by Matheis and Hickel³² for the large-scale turbulence-resolving CFD

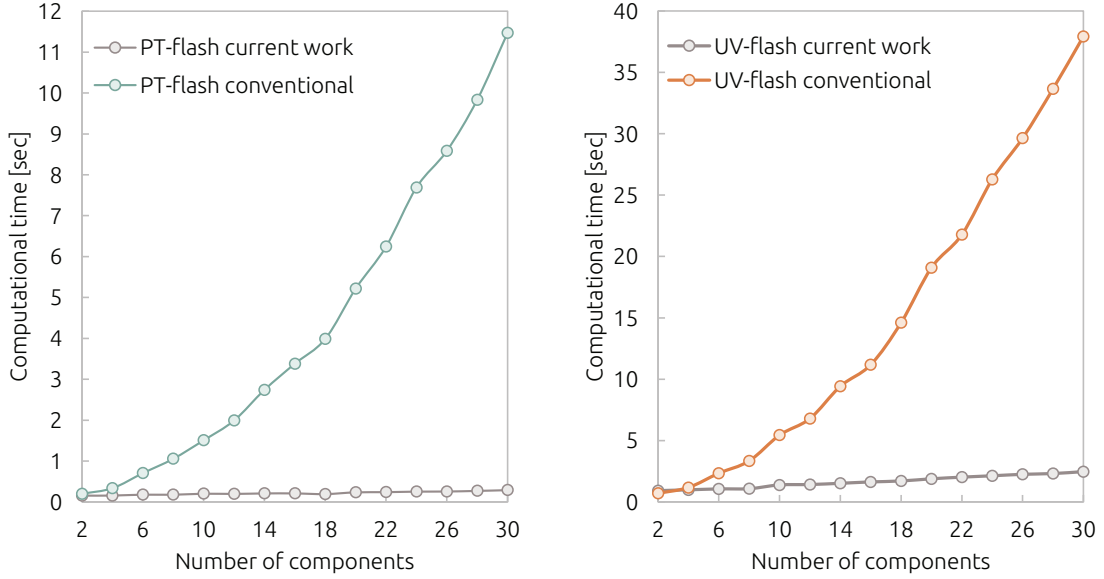


Figure 8: Computational time for PT-flashes and UV-flashes vs. number of mixture components. Shown is the total CPU time for 100×100 flash calculations in the part of the phase diagram highlighted in Fig. 7.

simulations of transcritical fuel injection. Both algorithms use a Newton method to achieve fast convergence. The calculations are performed on an Intel Xeon W-2123 CPU at 3.60 GHz and the Intel Fortran compiler was used.

The test fluid is a mixture of ethane and normal heptane. The phase diagrams of this binary mixture for various molar compositions are shown in Fig. 7. To study the effect of the component number in the mixture, we have added pseudo-components with properties identical to ethane and normal heptane and adjust the mole fractions in a way that the total composition remains constant. First, PT-flash calculations were carried out for a mixture with 26.54% ethane and we record the total computational time 100×100 states in the pressure-temperature range that is enclosed by the black box in Fig. 7. Then, the mixture internal energy and specific volume that were computed by the PT-flashes are used for executing the corresponding UV-flashes. In order to assess the performance of the proposed UV-flash at conditions that similar to what we typically encounter in CFD simulations, initial guesses of pressure and temperature were computed by adding random perturbations to the true values, that is:

$$T_{guess} = T_{true} + r\Delta T, \quad (76a)$$

$$p_{guess} = p_{true} + r\Delta p, \quad (76b)$$

where r is a random number generated in the range $[-0.5, 0.5]$. The perturbation amplitudes ΔT and Δp are set to 20 [K] and 20 kPa, which corresponds to the maximum change that we can expect between two subsequent time steps in CFD simulations.

The results are shown in Fig. 8. The computational time for the current PT-flash algorithm is always lower than the highly optimized reference method. The difference becomes more significant as the number of components is increased, which shows the importance of reduction methods for the both iso-thermal and non-isothermal flashes. Surprisingly, we also measure a performance gain for the two-component mixture, where the number of variables is not reduced by the new method. In this case, the reduction method acts as a preconditioner and reduces the number of required iterations for the PT-flash. Furthermore, it should be noted that the computational performance the UV-flash based on the VT-flash is much less sensitive to the amplitude of the imposed pressure perturbation Δp than the conventional method based on the PT-flash. For instance, the conventional method becomes more than five times slower for $\Delta p = 400$ kPa, whereas the overall time needed for the new method remains unchanged.

6 Discussion and Conclusions

This work was motivated by the need for computationally efficient and very robust vapor-liquid phase-split calculations in turbulence-resolving CFD simulations of high-pressure liquid-fuel injection and reacting transcritical multiphase flows in modern energy conversion systems, such as rocket engines, gas turbines and jet engines. Such simulations require typically 10^{10} to 10^{16} flash calculations for given overall specific internal energy, volume and composition and unknown pressure, temperature, volume fractions and phase compositions (isoenergetic-isochoric flash – UV-flash). The standard methods for such applications that we used in the past^{3,32} are based on a nested PT-flash and suffer from poor conditioning near the spinodal and coexistence curves and polynomial growth of the computational cost in terms of the number of mixture components. To this end, and building upon and extending the work of Mikyška and Firoozabadi¹⁶ and Nichita and Graciaa¹⁵, we have developed a new multi-component reduction method for direct PT-flash and VT-flash calculations based on the formulation of phase equilibrium conditions in terms of the molar specific value of Mikyška and Firoozabadi’s volume function and a corresponding adaptation of Nichita and Graciaa’s reduction method. The computational cost of solving the PT-flash and VT-flash in terms of the new reduced set of variables is almost independent of the number of components and the point in the phase diagram. The reduced-space Newton-Raphson iteration, using the exact analytical Ja-

cobian matrix, results in optimum quadratic convergence in very few iterations. We further showed that the non-isothermal UV and HP flashes are efficiently solved through univariate residual minimization with the naturally corresponding isothermal flash (PT-flash for HP-flash and VT-flash for UV-flash) and the specific heat capacity at constant pressure (for HP-flash) or at constant volume (for UV-flash) as exact Jacobian. We have thoroughly verified the reliability and efficiency of the algorithmic implementation. The computational results show a considerable speed-up compared to conventional methods, as well as improved robustness and better convergence behavior near the spinodal and coexistence curves of multi-component mixtures, where the preconditioning by the reduction method is most effective.

Acknowledgements

This work is funded by the Netherlands Organisation for Scientific Research (Contract No. 680.91.082).

References

1. Laurence Rongy, Kjetil B Haugen, and Abbas Firoozabadi. Mixing from Fickian diffusion and natural convection in binary non-equilibrium fluid phases. *AIChE Journal*, 58(5):1336–1345, 2012.
2. Ondej Polvka and Ji Mikyka. Compositional modeling in porous media using constant volume flash and flux computation without the need for phase identification. *Journal of Computational Physics*, 272:149 – 169, 2014.
3. Jan Matheis and Stefan Hickel. Multi-component vapor-liquid equilibrium model for LES of high-pressure fuel injection and application to ECN Spray A. *International Journal of Multiphase Flow*, 99:294–311, 2018.
4. Peter C. Ma, Hao Wu, Daniel T. Banuti, and Matthias Ihme. On the numerical behavior of diffuse-interface methods for transcritical real-fluids simulations. *International Journal of Multiphase Flow*, 113:231 – 249, 2019.
5. Carlos Rodriguez, Houman B Rokni, Foivos Koukouvinis, Ashutosh Gupta, and Manolis Gavaises. Complex multicomponent real-fluid thermodynamic model for high-pressure Diesel fuel injection. *Fuel*, 257:115888, 2019.

6. Principio Tudisco and Suresh Menon. Numerical Investigations of Phase-Separation During Multi-Component Mixing at Super-Critical Conditions. *Flow, Turbulence and Combustion*, 104 (2):(in press), 2020.
7. AS Abhvani, DN Beaumont, et al. Development of an efficient algorithm for the calculation of two-phase flash equilibria. *SPE Reservoir Engineering*, 2(04):695–702, 1987.
8. Michael L. Michelsen. Speeding up the two-phase PT-flash, with applications for calculation of miscible displacement. *Fluid Phase Equilibria*, 143(1):1 – 12, 1998.
9. Michael L Michelsen. The isothermal flash problem. Part I. Stability. *Fluid phase equilibria*, 9 (1):1–19, 1982.
10. Michael L Michelsen. The isothermal flash problem. Part II. Phase-split calculation. *Fluid phase equilibria*, 9(1):21–40, 1982.
11. Michael L Michelsen. State function based flash specifications. *Fluid Phase Equilibria*, 158: 617–626, 1999.
12. Michael L Michelsen. Simplified flash calculations for cubic equations of state. *Industrial & Engineering Chemistry Process Design and Development*, 25(1):184–188, 1986.
13. Martin Petitfrere and Dan Vladimir Nichita. A comparison of conventional and reduction approaches for phase equilibrium calculations. *Fluid Phase Equilibria*, 386:30–46, 2015.
14. EM Hendriks and ARD Van Bergen. Application of a reduction method to phase equilibria calculations. *Fluid Phase Equilibria*, 74:17–34, 1992.
15. Dan Vladimir Nichita and Alain Graciaa. A new reduction method for phase equilibrium calculations. *Fluid Phase Equilibria*, 302(1-2):226–233, 2011.
16. Jiří Mikyška and Abbas Firoozabadi. A new thermodynamic function for phase-splitting at constant temperature, moles, and volume. *AIChE Journal*, 57(7):1897–1904, 2011.
17. Tereza Jindrová and Jiří Mikyška. General algorithm for multiphase equilibria calculation at given volume, temperature, and moles. *Fluid Phase Equilibria*, 393:7–25, 2015.
18. Dan Vladimir Nichita. New unconstrained minimization methods for robust flash calculations at temperature, volume and moles specifications. *Fluid Phase Equilibria*, 466:31–47, 2018.

19. Martin Cismondi, Papa Matar Ndiaye, and Frederico W Tavares. A new simple and efficient flash algorithm for Tv specifications. *Fluid Phase Equilibria*, 464:32–39, 2018.
20. Abbas Firoozabadi. *Thermodynamics and Applications of Hydrocarbons Energy Production*. McGraw-Hill Professional, 2015.
21. Michael Locht Michelsen and Jørgen Mollerup. *Thermodynamic Models: Fundamentals and Computational Aspects*. Tie-Line Publications, 2007.
22. Dan Vladimir Nichita and Martin Petitfrere. Phase stability analysis using a reduction method. *Fluid Phase Equilibria*, 358:27–39, 2013.
23. Elke Goos, Alexander Burcat, and Branko Ruscic. Third millennium ideal gas and condensed phase thermochemical database for combustion. *URL: <http://garfield.chem.elte.hu/Burcat/burcat.html>*, 2009.
24. Jiří Mikyška and Abbas Firoozabadi. Investigation of mixture stability at given volume, temperature, and number of moles. *Fluid Phase Equilibria*, 321:1–9, 2012.
25. Dan Vladimir Nichita. Fast and robust phase stability testing at isothermal-isochoric conditions. *Fluid Phase Equilibria*, 447:107–124, 2017.
26. Dan Vladimir Nichita and Claude F Leibovici. A rapid and robust method for solving the Rachford–Rice equation using convex transformations. *Fluid Phase Equilibria*, 353:38–49, 2013.
27. Lyman Yarborough. Vapor-liquid equilibrium data for multicomponent mixtures containing hydrocarbon and nonhydrocarbon components. *Journal of Chemical and Engineering Data*, 17(2):129–133, 1972.
28. Richard S Metcalfe and Lyman Yarborough. The effect of phase equilibria on the CO₂ displacement mechanism. *SPE Journal*, 19(04):242–252, 1979.
29. Abbas Firoozabadi and Huanquan Pan. Fast and robust algorithm for compositional modeling: Part I - stability analysis testing. *SPE Journal*, 7(1):78–89, 2002.
30. W B Kay. Liquid-vapor phase equilibrium relations in the Ethane- n-Heptane system. *Industrial and Engineering Chemistry*, 30(4):459–465, April 1938.
31. Vinod S Mehra and George Thodos. Vapor-liquid equilibrium in the Ethane-n-Heptane system. *Journal of Chemical and Engineering Data*, 10(3):211–214, July 1965.

32. Jan Matheis and Stefan Hickel. Multi-component vapor-liquid equilibrium model for LES and application to ECN Spray A. In *Studying Turbulence Using Numerical Simulation Databases - XVI - Proceedings of the 2016 Summer Program*, pages 25–34. Center for Turbulence Research, Stanford University, 2016.